PCCP

PAPER

View Article Online
View Journal | View Issue

Cite this: *Phys. Chem. Chem. Phys.*, 2016, **18**, 25687

Hydrogen evolution from water using Mo–oxide clusters in the gas phase: DFT modeling of a complete catalytic cycle using a $Mo_2O_4^-/Mo_2O_5^-$ cluster couple

Manisha Ray, Arjun Saha and Krishnan Raghavachari*

Received 17th June 2016,
Accepted 22nd August 2016

DOI: 10.1039/c6cp04259g

www.rsc.org/pccp

Density functional theory (DFT) calculations using a small metal cluster couple, $Mo_2O_4^-/Mo_2O_5^-$, are used to model a complete catalytic cycle for H_2 production from water. While $Mo_2O_4^-$ is known to readily react with water to form $Mo_2O_5^-$ and release H_2, the principal challenge is in reducing $Mo_2O_5^-$ to $Mo_2O_4^-$ to complete the cycle. We investigate the role of several potential sacrificial reagents (ethylene, propylene, CO and acetylene) that can reduce $Mo_2O_5^-$ after the initial oxidation. DFT calculations of the free energy reaction pathways demonstrate the presence of overall kinetically accessible barriers that are below the entrance channel (separated reactants) in the $Mo_2O_4^-$ + H_2O reaction (step I) followed by the $Mo_2O_5^-$ + sacrificial reagent reactions (step II). Though the overall reaction is thermodynamically favorable, the first step is highly exothermic while the second step is endothermic. The deepest part of the potential energy surface is a complex of $Mo_2O_5^-$ with the sacrificial reagent. If the energy gained in the first reaction and the succeeding complex formation is not lost due to collisions, the subsequent barriers can be overcome, leading to possible catalytic applications of the $Mo_2O_4^-/Mo_2O_5^-$ cluster couple in H_2 production reactions.

Introduction

Transition metal oxides (TMOs) are known to be involved in many bond activation reactions (C–H, O–H and C–O) for both catalytic and non-catalytic applications.[1–6] Over the last several years, TMOs as bare or incorporated with other materials play a very important role in the area of heterogeneous catalysis.[7] For example, the use of TMOs as semiconductor surfaces for photo-electrochemical water splitting to produce hydrogen (H_2) has attracted considerable attention.[8–10] Hydrogen, as an alternative energy source, is expected to be a possible replacement of fossil fuels that cause undesired emission from their combustion in the environment.

Determining the molecular scale interactions in metal oxide surface catalysis continues to pose major challenges. Many factors such as surface inhomogeneity almost always add to the complexity in such studies, and often prevent the understanding of the intrinsic features of the reactions. Small gas phase clusters have often been suggested as well defined models of the active sites on such surfaces which can enable us to understand the essential factors that govern their reactive behavior.[11–18] Taking into account the importance of TMOs' participation in H_2 production, we have carried out theoretical and experimental investigations (in collaboration with the Jarrold group) of the reactions of small molybdenum and tungsten metal oxide cluster anions with water to release H_2.[19–21] In particular, metal-rich cluster anions of the Mo/W oxides ($M_xO_y^-$, M = Mo, W, x = 2–4, $y < 3x$) have been considered in such studies.

DFT calculated reaction pathways obtained by our group have determined that a high kinetic barrier for producing H_2 is present in the metal oxide clusters when the metal reaches a high oxidation state during the course of the reaction.[22,23] Typically, the reactions lead to sequential oxidation (accompanied by H_2 release) up to a point and then terminate with an adduct formation. For example, in the bimetallic $Mo_2O_y^-$ series, reactions of reduced clusters (y = 2–4) with water successfully lead to hydrogen production, but terminate with a product of water addition when the metal centers are saturated and unlikely to react further. The strength of the metal–oxygen bond makes such reactions highly exothermic, thereby making them irreversible without the introduction of additional energy. Therefore, in order to complete a genuine catalytic cycle of H_2 production, the resulting highly oxidized clusters from $Mo_xO_y^-/W_xO_y^-$ + H_2O reactions have to be reduced using reagents, commonly known as sacrificial reagents, so that the reduced cluster can further react with another molecule of H_2O and, therefore, maintain a complete cycle of H_2 production.

The potential applicability of Mo–oxide systems towards hydrocarbon oxidation[24–26] *via* C–H bond activation indicates that

Department of Chemistry, Indiana University, 800 E Kirkwood Avenue, Bloomington, IN 47405, USA. E-mail: kraghava@indiana.edu

Table 1 Enthalpies (298 K) of several H_2O reduction reactions by ethylene (C_2H_4), propylene (C_3H_6), CO and acetylene (C_2H_2). Data derived from experimental heats of formation from the NIST thermochemical database[a]

Reaction	ΔH_{298} (kcal mol^{-1})
$CH_2{=}CH_2 + H_2O \rightarrow CH_3CHO + H_2$	+4.5
$CH_3CH{=}CH_2 + H_2O \rightarrow (CH_3)_2CO + H_2$	+0.7
$CO + H_2O \rightarrow CO_2 + H_2$	−9.8
$CH{\equiv}CH + H_2O \rightarrow CH_2CO + H_2$	−17.2

[a] For C_2H_4, C_2H_2 and CO: C. M. W. Chase, Jr., *NIST-JANAF Themochemical Tables, Fourth Edition*, *J. Phys. Chem. Ref. Data, Monograph 9*, 1998, 1–1951; for C_3H_6: S. Furuyama, D. M. Golden, S. W. Benson, *J. Chem. Thermodyn.*, 1969, **1**, 363–375, data from NIST Standard Reference Database 69: NIST Chemistry WebBook. http://webbook.nist.gov/chemistry/.

several alkenes and/or alkynes (ethylene, acetylene, and their substituted systems) can potentially be used as sacrificial reagents to reduce the Mo–oxide clusters. Indeed, alkene/alkyne oxidation reactions through C–C/C–H bond activations are fundamentally and industrially important processes.[27–32] Thus, our primary goal in the present study is to explore the extent to which Mo–oxide clusters can be used as catalysts for H_2 production in water reduction reactions by using sacrificial reagents. We only consider sacrificial reagents that undergo thermodynamically feasible (exothermic or close to thermoneutral, see Table 1) H_2 elimination reactions from water in combined oxidation–reduction reactions.

In this study, we have chosen the $Mo_2O_4^-/Mo_2O_5^-$ small cluster couple in the bimetallic Mo–oxide cluster series as the model system to investigate the full catalytic cycle. The starting $Mo_2O_4^-$ cluster is not highly oxygen deficient, preventing multiple oxidation steps with water. However, it does readily react in one step; the $Mo_2O_5^-$ cluster is produced by the $Mo_2O_4^-$ + H_2O reaction accompanied by H_2 production. In the following sections, using DFT, we report extensive calculations on the $Mo_2O_5^-$ + several sacrificial hydrocarbon reagents (ethylene, propylene, and acetylene) that might reduce the cluster, thus providing a complete cycle for H_2 formation. Finally, considering the thermodynamic availability of the well-known water–gas shift reaction, we have also explored this reaction using $Mo_2O_4^-/Mo_2O_5^-$ clusters, where CO will play the role of the sacrificial reagent in reducing $Mo_2O_5^-$ to $Mo_2O_4^-$.

Results and discussion

The DFT calculated reaction energy profiles for H_2O reduction by several hydrocarbons (C_2H_4, CH_3–$CH{=}CH_2$, C_2H_2) and CO in the presence of the $Mo_2O_4^-/Mo_2O_5^-$ cluster couple are shown in Fig. 1 and 2. A complete potential energy profile for catalytic H_2 production includes PES I for water reduction by the $Mo_2O_4^-$ cluster followed by PES II for the oxidation of a second reactant by $Mo_2O_5^-$ to regenerate $Mo_2O_4^-$. Briefly, previous calculations on the $Mo_2O_4^-$ + H_2O reaction[23] predicted low sequential kinetic barriers throughout the reaction coordinate, readily leading to H_2 production. The end product of the $Mo_2O_4^-$ + H_2O reaction is a $Mo_2O_5^-$ cluster with a high internal energy (stabilized by approximately 50 kcal mol^{-1} compared to the initial reactants), as shown in Fig. 1 and 2. Under collision-free conditions, it is thus possible

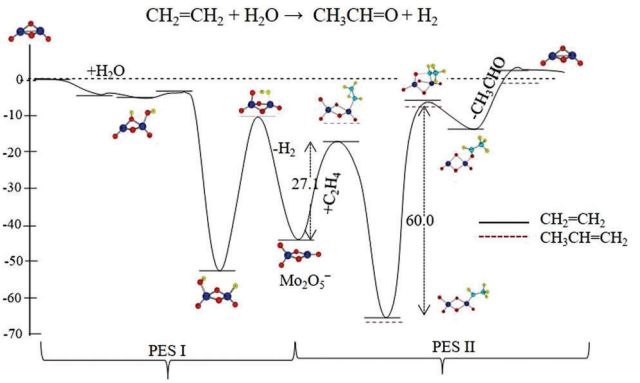

Fig. 1 Free energy reaction profiles (PES I and PES II) calculated using the M06 density functional for the reduction of H_2O by ethylene ($CH_2{=}CH_2$) and propylene (CH_3–$CH{=}CH_2$) in the presence of the $Mo_2O_4^-/Mo_2O_5^-$ cluster couple. Relative energies (kcal mol^{-1}) of all the species are calculated from the separated reactants at the entrance channel.

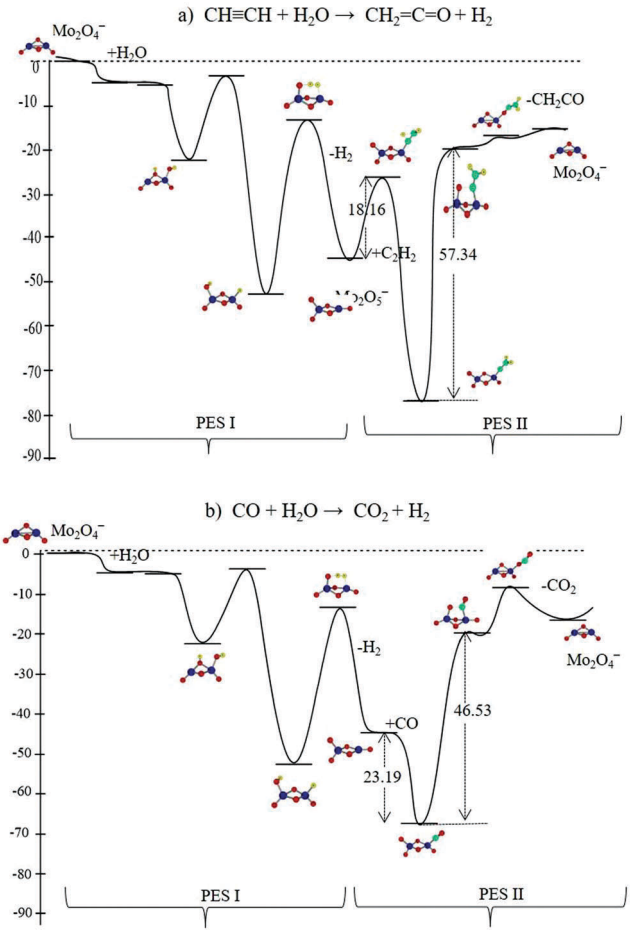

Fig. 2 Free energy reaction profiles (PES I and PES II) for H_2O reduction by (a) acetylene (CH≡CH) and (b) CO in the presence of the $Mo_2O_4^-/Mo_2O_5^-$ cluster couple. Relative energies (kcal mol^{-1}) of the species are calculated from the separated reactants at the entrance channel.

that $Mo_2O_5^-$ can further potentially interact with a second reactant *via* PES II reducing $Mo_2O_5^-$ to $Mo_2O_4^-$, resulting in a complete catalytic cycle.

In PES II, the reduction of $Mo_2O_5^-$ occurs through the initial binding of the C atom of C_2H_4, C_2H_2 or CO to the Mo atom of $Mo_2O_5^-$. The repulsive negative electrostatic potential (ESP) around these anionic clusters [as shown in Fig. 4(b)] primarily limits the interaction of these nucleophilic molecules (C_2H_4, C_2H_2 or CO) to the less coordinated metal atom instead of favorable interactions that are possible from an initial cluster with positive ESP. For example, the mechanism of CO binding to $Mo_2O_5^-$ is typically rationalized by electron donation from the HOMO π-type orbital of CO to the empty metal d-orbital and back donation from the filled metal d-orbital to the π^* LUMO of CO. The resulting strong metal–carbon bond formation stabilizes these nucleophilic addition complexes by around 70 kcal mol^{-1}, relative to the initial reactants for all the sacrificial reagents considered here. The energy of formation of a 2nd carbon–oxygen bond is also below that of the initial separated reactants, but comparatively higher in terms of stabilization energy gained in the previous step due to the dissociation of a high energy Mo–O bond.

The nucleophilic addition complex is the most stable species (~ -80 kcal mol^{-1}) in the entire reaction pathway due to the formation of a high energy metal–carbon bond and, therefore, resides in a deep potential well, as can be seen in all the energy profiles. It is interesting to note that all the barriers calculated in PES II pathways are consistently lower than the entrance channel energies of the separated reactants. However, it is also important to note that, in contrast to PES I, each of the calculated barriers in PES II are sequentially higher than the addition complex, and they reasonably exceed the internal energy gained by the preceding intermediates. This trend has been observed for all the PES II pathways as depicted in Fig. 1, which indicates that the internal energy should remain very high throughout the overall course of the reaction in order to allow the second reaction to occur.

The sequential presence of comparatively high barriers in the reaction pathway (PES II) might result in the termination of the reaction at the M–C bound complex without resulting in a complete catalytic cycle. The least favorable systems in $Mo_2O_5^-$ reduction are ethylene and propylene [Fig. 1], where the formation of a second carbon–oxygen bond involves an energy barrier of 60 kcal mol^{-1}. The overall product formation is, however, found to be nearly thermoneutral or slightly endothermic for these two systems. This is consistent with the known thermodynamic values for the ethylene and propylene reactions listed in Table 1.

The reactions with CO and acetylene are more thermodynamically favorable as seen in Table 1. This is consistent with the comparatively low kinetic barriers in PES II for $Mo_2O_5^-$ + acetylene/CO reactions that result in exothermic product formation in PES II in Fig. 2(a) and (b). In the $Mo_2O_5^-$ + CO reaction, $Mo_2O_5^-$ is further stabilized by 23 kcal mol^{-1} when bonded to a CO molecule *via* an addition complex that forms without a barrier. In contrast, in the $Mo_2O_5^-$ + acetylene reaction, the addition complex forms with a barrier of 18 kcal mol^{-1} that is readily accessible by $Mo_2O_5^-$ in the pathway. However, in both these systems, the formation of a second carbon–oxygen bond in the final intermediate requires an activation energy of around 50 kcal mol^{-1} from the addition complex to surmount the barrier.

In an effort to understand the elimination of CO_2 and CH_2CO from the final intermediate in $Mo_2O_5^-$ + CO/acetylene reactions *via* PES II, both the structure and bonding scenarios have been investigated in the final intermediate. The stretching of the Mo–O bond length in the linear $Mo_2O_4(CO_2)^-$ and $Mo_2O_4(CH_2CO)^-$ intermediates from 1.71 Å to 1.95–2.03 Å is consistent with the possible breaking of the Mo–O bond and the oxidation of CO (or acetylene) to CO_2 (or CH_2CO). The increased bond length that promotes the breaking of a metal–oxygen bond in oxidation reactions of unsaturated hydrocarbons or CO is frequently observed in metal oxide species containing a radical oxygen center (M–$O^\bullet$).[33–35] The formation of such $O^{-\bullet}$ active sites has not been observed in the $Mo_2O_5^-$–CO/acetylene intermediates studied in this report. However, our analysis suggests that the strong π–π molecular orbital (Fig. 3) overlap between C and O in the final intermediate contributes to the weakening of the Mo–O bond in order to reduce the cluster intermediate participating in CO/acetylene oxidations.

Remarkable effects on reactivity trends have been observed for metal clusters when both reactants in such dual reactant reaction environments are exposed to the clusters either simultaneously or sequentially.[36] It is reported that in a sequential reaction environment, the pre-adsorption of one reactant on the cluster results in an increased reactivity by a modification of the electronic structure and properties of the adsorbent in order to appear electronically different to the second reactant. This is exactly what has been observed in the PES I of $Mo_2O_4^-$ + H_2O reaction, where the $Mo_2O_5^-$ cluster attains high internal energy through the formation of a strong Mo–O bond from the reaction of H_2O with $Mo_2O_4^-$. The internal energy gained drives $Mo_2O_5^-$ to further react with CO/C_2H_2 in PES II.

To illustrate the point about the internal energy gained by the $Mo_2O_5^-$ in the first step (PES I) *via* $Mo_2O_4^-$ + H_2O reaction, we have shown the steps involved in the elementary $Mo_2O_5^-$ + CO reaction separately in Fig. 4(a). The reaction involves a stable initial $Mo_2O_5^-$·CO complex followed by a high kinetic barrier to the formation of a new C–O bond along the reaction pathway. The barrier exceeds the entrance channel energy significantly,

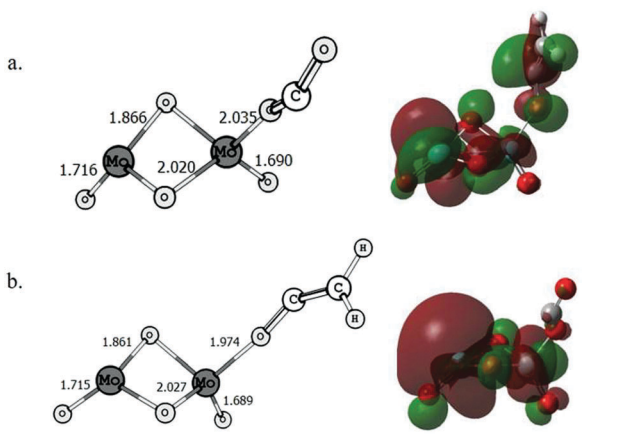

Fig. 3 Structural parameters (bond lengths) in the final intermediate of $Mo_2O_5^-$ + CO and $Mo_2O_5^-$ + C_2H_2 reactions in PES II. The corresponding HOMOs (Highest Occupied Molecular Orbitals) are also shown.

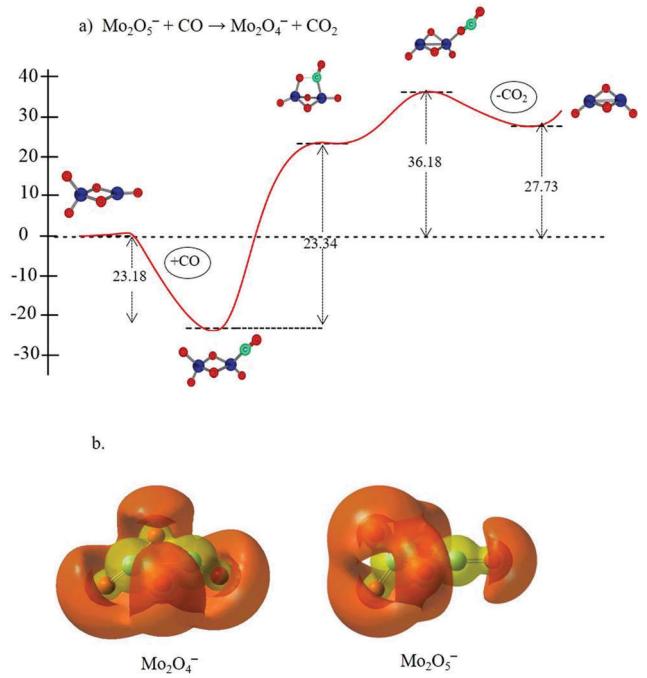

Fig. 4 (a) Calculated free energy profile for the elementary reaction, $Mo_2O_5^-$ + CO and (b) calculated molecular electrostatic potentials (MEPs) for the anionic $Mo_2O_4^-$ and $Mo_2O_5^-$, where orange corresponds to negative charge and yellow corresponds to positive charge.

resulting either in no reaction or only the formation of an electrostatic complex $Mo_2O_5^-$·CO. This supports the experimentally favored metal carbonyl complex formation over CO oxidation in the $Mo_2O_y^-$ + CO reaction as observed by Jarrold *et al.* in mass spectrometric studies followed by photoelectron spectroscopy on the metal–carbonyl complexes.[37,38] Thus, the reaction can proceed to regenerate $Mo_2O_4^-$ only if the internal energy from the first step is maintained under low collision conditions in such gas phase experimental studies.

To summarize, the key observation in these reactions is the presence of a highly stabilized CO/C_2H_2 addition complex resulting in a high subsequent activation barrier that needs to be overcome by the complex to complete the reduction of $Mo_2O_5^-$ *via* PES II. In a study of CO oxidation by several anionic 1st row TMO clusters (Fe, Co, Ni and Cu), the Castleman group has shown that the large initial CO binding energies (where C is directly bonded to the metal) enable the reaction complex to overcome any subsequent barriers to CO oxidation, supported by their experimentally observed products.[39–41] However, the reactivity rates were quite different for several clusters that depend on the spin state preservation in the calculated pathway as revealed by their PES calculations. In the present study, the calculated PES II for oxidation of the CO/C_2H_2 by the $Mo_2O_5^-$ cluster shows a similar trend of complex formation, though there is a change in the spin state of the ground state structures from quartet (for $Mo_2O_4^-$) in the reactant to doublet (for $Mo_2O_5^-$) in the product.

A spin state change in a reaction due to spin–orbit coupling between two wave functions corresponding to different spins is very common in transition metal chemistry. Reactions that preserve the same spin multiplicity from reactants to products frequently show thermodynamic preference throughout the reaction pathway as previously observed in several DFT studies on the reactions of transition metal oxides with small molecules.[39,42–44] The reaction exothermicity is primarily determined by the position of the minimum energy crossing point (MECP) between the potential energy surfaces corresponding to two different spin states. A spin forbidden reaction can often be exothermic when the MECP lies in the immediate vicinity of the minimum corresponding to the lowest energy spin state.[45–47]

In a previous study on the reactions of 1st row TMOs (Cobalt) with CO, Castleman and coworkers[39] have observed that the initial binding of CO is associated with the spin crossover. In contrast, in the case of $Mo_2O_5^-$ + CO reaction, the spin crossover occurs during the structural rearrangement between $Mo_2O_5^-$–CO and $Mo_2O_4^-$–OCO complexes. In addition to the spin crossover, we expect that the MECP for this reaction will be followed by a high barrier to the quartet $Mo_2O_4^-$–OCO minimum (which may lead to slow reactivity), but the primary rate-determining step for reducing the $Mo_2O_5^-$ cluster by CO in this reaction is the high energy TS that undergoes strong metal–oxygen bond dissociation during rearrangement. While a spin-crossover is thus required, the thermodynamic availability of the final products and the kinetic barriers in PES II for these reactions are quite similar to the reactions reported by Castleman's group for 1st row TMOs with CO. These observations certainly indicate that the presence of internal energy may be sufficient to overcome the barriers to complete the catalytic cycle. However, the reactivity of the $Mo_2O_5^-$ cluster might be very low due to the high kinetic barriers in addition to the inversion of spin in the PES II which will indirectly affect H_2 production using $Mo_2O_4^-$/$Mo_2O_5^-$ as a catalyst in this H_2O reduction by either CO or acetylene.

An enhanced reactivity and selectivity to gas phase CO or unsaturated hydrocarbon oxidation were investigated for metal oxide clusters that contain a radical oxygen center. Johnson *et al.*[33,34] have reported that the nature of the charges on metal oxide clusters primarily influences the catalytic activity irrespective of the presence of the radical center in both cationic and anionic Zr–oxide clusters. A different molecular electrostatic potential (MEP) around the anionic and cationic metal oxide clusters was suggested to be primarily responsible for their different reactivity with several nucleophiles such as CO, acetylene or ethylene. The negative MEP around the anionic cluster repels the approach of nucleophiles and results in a very high kinetic barrier in such reactions, compared to the easily surmountable barriers for cationic Zr–oxide clusters. The MEP for $Mo_2O_5^-$ or $Mo_2O_4^-$ clusters is shown in Fig. 4(b). The negative MEP is comparatively lower for $Mo_2O_4^-$ due to the lower number of oxygen atoms around the metal atoms. This may contribute partly to the comparatively low barriers in PES I for H_2 production, but high barriers for subsequent CO or C_2H_2 oxidation by $Mo_2O_5^-$ in PES II.

In summary, we aim to provide insights into the H_2 production reaction in a complete catalytic cycle using the model $Mo_2O_4^-$/$Mo_2O_5^-$ cluster couple through DFT calculations. A schematic diagram of the overall reactions is shown in Fig. 5. Regardless of the highly favorable H_2 production from $Mo_2O_4^-$ + H_2O reaction,

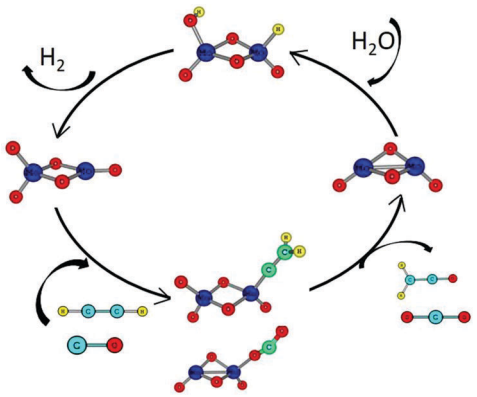

Fig. 5 A schematic diagram of the possible catalytic cycle for H_2 production using the model system $Mo_2O_4^-/Mo_2O_5^-$ cluster couple.

our calculations predict a high barrier for $Mo_2O_5^-$ reduction by CO/C_2H_2 in the $Mo_2O_4^-/Mo_2O_5^-$ cycle. The presence of internal energy from the first step will play a key role in the completion of the catalytic step. If there is a slight loss in the internal energy, the input of external energy by increasing the temperature or *via* collisional activation might be a useful strategy to complete the catalytic cycle, as in many catalytic reactions that do not occur at room temperature.[48] Also, Mo–oxide mixed with 1st row or 2nd row transition metal oxides may be interesting systems for H_2 production since mixed metal oxides often show higher reactivity and selectivity than their pure single metal oxide analogues.[49,50]

Conclusions

In conclusion, we have carried out a study on the catalytic application of group 6 transition metal oxide clusters for H_2 production *via* gas phase reactions. We have computationally demonstrated the possible reduction of the $Mo_2O_5^-$ cluster by several reducing reagents – C_2H_4, C_3H_6, C_2H_2 and CO – in order to complete the cycle of H_2 production from the $Mo_2O_4^- + H_2O$ reaction that produces $Mo_2O_5^-$ and H_2. Of the several reagents explored, the lowest reactivity towards $Mo_2O_5^-$ reduction has been observed for C_2H_4 and C_3H_6, while C_2H_2 and CO show thermodynamically and kinetically available final product formation in the calculated pathways. Regardless of the thermodynamic availability of the final product formation calculated in the complete potential energy profile, PES II is significantly endothermic with a high kinetic barrier of about 50 kcal mol^{-1} for CO/C_2H_2 oxidation. In addition, initial large binding energies of the addition complex of $Mo_2O_5^-$ with the sacrificial reagent should also be considered, though the subsequent high barriers are still below the entrance channel energy. Therefore, under low collision reaction conditions, it is possible that the energy gained in PES I and succeeding complex formation might be large enough to overcome any subsequent barriers, and could lead to possible catalytic applications of the $Mo_2O_4^-/Mo_2O_5^-$ cluster couple in H_2 production reactions. It may also be possible to input external energy to overcome the partial loss of energy due to collisions. Notwithstanding the limitations of the study, further investigations on several Mo–oxide or mixed metal oxide clusters will be helpful to study their role in many catalytic reactions.

Computational methods

The potential energy pathways for all the reactions were investigated using Gaussian 09 suite of electronic structure programs.[51] To accurately determine the reaction free energies for each species along the computed pathways, the hybrid M06 density functional was employed due to its overall good performance in similar reaction systems.[52,53] A Stuttgart–Dresden relativistic pseudopotential was used to replace the 28 core electrons, and an augmented version of the associated double-ζ basis set containing diffuse and polarization functions was used for geometry optimizations of all the minima and transition states.[54] Vibrational frequency analysis was conducted at each stationary point to ensure the nature of the minima and transition states. Intrinsic reaction coordinate (IRC) calculations were also performed to connect the transition state to the minima reported in the calculated pathways.

In order to get accurate relative energies of the stationary points, single point calculations were carried out using larger triple-ζ quality basis sets for Mo augmented with two f-type functions ($\zeta_f = 0.338, 1.223$) and one g-type function ($\zeta_g = 0.744$), as described by Martin and Sundarmann.[55] Furthermore, diffuse s-, p-, and d-functions were added to the Mo-basis set (with an exponent ratio of 0.3) to properly describe the increased radial extent of the anions. C, H and O atoms were treated with Dunning's correlation-consistent basis set (aug-cc-pVTZ). The relative free energies (G) along the reaction energy path at 298 K were calculated by taking the free energy difference between different stationary points and infinitely separated reactants.

Acknowledgements

This work was supported in its entirety by the Department of Energy Grant No. DE-FG02-07ER15889.

References

1 Z.-C. Wang, S. Yin and E. R. Bernstein, *Phys. Chem. Chem. Phys.*, 2013, **15**, 10429–10434.
2 V. Blagojevic, G. Orlova and D. K. Bohme, *J. Am. Chem. Soc.*, 2005, **127**, 3543–3555.
3 D. K. Bohme and H. Schwarz, *Angew. Chem., Int. Ed.*, 2005, **44**, 2336–2354.
4 K. A. Zemski, D. R. Justes and A. W. Castleman, Jr., *J. Phys. Chem. B*, 2002, **106**, 6136–6148.
5 Y. Xie, F. Dong, S. Heinbuch, J. J. Rocca and E. R. Bernstein, *J. Chem. Phys.*, 2009, **130**, 114306.
6 S. Yin, Z. Wang and E. R. Bernstein, *J. Chem. Phys.*, 2013, **139**, 084307.
7 D. E. Wilcox, *Chem. Rev.*, 1996, **96**, 2435–2458.
8 M. G. Walter, E. L. Warren, J. R. Mckone, S. W. Boettcher, Q. Mi, E. A. Santor and N. S. Lewis, *Chem. Rev.*, 2010, **110**, 6446–6473.

9 A. Fernando, K. L. Dimuthu, M. Weerawardene, N. V. Karimova and C. M. Aikens, *Chem. Rev.*, 2015, **115**, 6112–6216.
10 A. C. Reber, S. N. Khanna, P. J. Roach, W. H. Woodward and A. W. Castleman Jr, *J. Phys. Chem. A*, 2010, **114**, 6071–6081.
11 A. W. Castleman Jr. and S. N. Khanna, *J. Phys. Chem. C*, 2009, **113**, 2664–2674.
12 L. B. Pandey and C. M. Aikens, *J. Phys. Chem. A*, 2012, **116**, 526–535.
13 C. Lee and C. M. Aikens, *J. Phys. Chem. A*, 2014, **118**, 598–605.
14 A. Fernando, T. Haddock and C. M. Aikens, *J. Phys. Chem. A*, 2016, **120**, 2480–2492.
15 L. S. Wang, H. Wu and S. R. Desai, *Phys. Rev. Lett.*, 1996, **76**, 4853–4856.
16 P. Li, D. E. Miser, S. Rabiei, R. T. Yadav and M. R. Hajaligol, *Appl. Catal., B*, 2003, **43**, 151–162.
17 B. V. Reddy, F. Rasouli, M. R. Hajaligol and S. N. Khanna, *Chem. Phys. Lett.*, 2004, **384**, 242–245.
18 P. J. Roach, W. H. Woodward, A. W. Castleman Jr., A. C. Reber and S. N. Khanna, *Science*, 2009, **323**, 492–495.
19 D. W. Rothgeb, E. Hossain, A. T. Kuo, J. L. Troyer, C. C. Jarrold, N. J. Mayhall and K. Raghavachari, *J. Chem. Phys.*, 2009, **130**, 124314.
20 D. W. Rothgeb, J. Mann and C. C. Jarrold, *J. Chem. Phys.*, 2010, **133**, 054305.
21 D. W. Rothgeb, E. Hossain, J. E. Mann and C. C. Jarrold, *J. Chem. Phys.*, 2010, **131**, 064302.
22 N. J. Mayhall, D. W. Rothgeb, E. Hossain, C. C. Jarrold and K. Raghavachari, *J. Chem. Phys.*, 2009, **131**, 144302.
23 M. Ray, S. E. Waller, A. Saha, K. Raghavachari and C. C. Jarrold, *J. Chem. Phys.*, 2014, **141**, 104310.
24 N. J. Mayhall and K. Raghavachari, *J. Phys. Chem. A*, 2007, **111**, 8211–8217.
25 T. Waters, A. J. Richard O'Hair and G. Anthony Wedd, *J. Am. Chem. Soc.*, 2003, **125**, 3384–3396.
26 G. Fu, X. Xu, X. Lu and H. Wan, *J. Am. Chem. Soc.*, 2005, **127**, 3989–3996.
27 J. H. Lunsford, *Catal. Today*, 2000, **63**, 165–174.
28 J. A. Labinger and J. E. Bercaw, *Nature*, 2002, **417**, 507–514.
29 S. Sahoo, A. C. Reber and S. N. Khanna, *J. Phys. Chem. A*, 2015, **119**, 12855–12861.
30 Z. C. Wang, S. Yin and E. R. Bernstein, *J. Phys. Chem. A*, 2013, **117**, 2294–2301.
31 F. Dong, S. Heinbuch, Y. Xie, E. R. Bernstein, J. J. Rocca, Z.-C. Wang, X.-L. Ding and S.-G. He, *J. Am. Chem. Soc.*, 2009, **131**, 1057–1066.
32 S. Yin, Y. Xie and E. R. Bernstein, *J. Phys. Chem. A*, 2011, **115**, 10266–10275.
33 G. E. Johnson, R. Mitrić, M. Nössler, E. C. Tyo, V. Bonačić-Koutecký and A. W. Castleman Jr., *J. Am. Chem. Soc.*, 2009, **131**, 5460–5470.
34 G. E. Johnson, R. Mitrić, E. C. Tyo, V. Bonačić-Koutecký and A. W. Castleman, Jr., *J. Am. Chem. Soc.*, 2008, **130**, 13912–13920.
35 A. Fernando and C. M. Aikens, *Phys. Chem. Chem. Phys.*, 2015, **17**, 32443–32454.
36 W. T. Wallace and R. L. Whetten, *J. Am. Chem. Soc.*, 2002, **124**, 7499–7505.
37 E. Hossain and C. C. Jarrold, *J. Chem. Phys.*, 2009, **130**, 064301.
38 R. B. Wyrwas, E. M. Robertson and C. C. Jarrold, *J. Chem. Phys.*, 2007, **126**, 214309.
39 J. U. Reveles, G. E. Johnson, S. N. Khanna and A. W. Castleman, *J. Phys. Chem. C*, 2010, **114**, 5438–5446.
40 N. M. Reilly, J. U. Reveles, G. E. Johnson, J. M. del Campo, S. N. Khanna, A. M. Köster and A. W. Castleman, Jr., *J. Phys. Chem. C*, 2007, **111**, 19086–19097.
41 B. V. Reddy, F. Rasoulia, M. R. Hajaligola and S. N. Khanna, *Fuel*, 2004, **83**, 1537–1541.
42 R. Burgert, H. Schnockel, A. Grubisic, X. Li, S. T. Stokes, K. H. Bowen, G. F. Ganteför, B. Kiran and P. Jena, *Science*, 2008, **319**, 438–442.
43 N. M. Reilly, J. U. Reveles, G. E. Johnson, S. N. Khanna and A. W. Castleman, Jr., *J. Phys. Chem. A*, 2007, **111**, 4158–4166.
44 N. M. Reilly, J. U. Reveles, G. E. Johnson, S. N. Khanna and A. W. Castleman, Jr., *Chem. Phys. Lett.*, 2007, **435**, 295–299.
45 N. Strickland and J. N. Harvey, *J. Phys. Chem. B*, 2007, **111**, 841–852.
46 J.-L. Carreón-Macedo and J. N. Harvey, *J. Am. Chem. Soc.*, 2004, **126**, 5789–5797.
47 C. J. Cramer and D. G. Truhlar, *Phys. Chem. Chem. Phys.*, 2009, **11**, 10757–10816.
48 B. Chiavarino, M. E. Crestoni and S. Fornarini, *Chem. – Eur. J.*, 2002, **8**, 2740–2746.
49 M. Sadakane, N. Watanabe, T. Katou, Y. Nodasaka and W. Ueda, *Angew. Chem., Int. Ed.*, 2007, **46**, 1493–1496.
50 G. Mestl, *Top. Catal.*, 2006, **38**, 69–82.
51 M. J. Frisch, G. W. Trucks, H. B. Schlegel, G. E. Scuseria, M. A. Robb, J. R. Cheeseman, G. Scalmani, V. Barone, B. Mennucci, G. A. Petersson, H. Nakatsuji, M. Caricato, X. Li, H. P. Hratchian, A. F. Izmaylov, J. Bloino, G. Zheng, J. L. Sonnenberg, M. Hada, M. Ehara, K. Toyota, R. Fukuda, J. Hasegawa, M. Ishida, T. Nakajima, Y. Honda, O. Kitao, H. Nakai, T. Vreven, J. A. Montgomery, Jr., J. E. Peralta, F. Ogliaro, M. Bearpark, J. J. Heyd, E. Brothers, K. N. Kudin, V. N. Staroverov, R. Kobayashi, J. Normand, K. Raghavachari, A. Rendell, J. C. Burant, S. S. Iyengar, J. Tomasi, M. Cossi, N. Rega, J. M. Millam, M. Klene, J. E. Knox, J. B. Cross, V. Bakken, C. Adamo, J. Jaramillo, R. Gomperts, R. E. Stratmann, O. Yazyev, A. J. Austin, R. Cammi, C. Pomelli, J. W. Ochterski, R. L. Martin, K. Morokuma, V. G. Zakrzewski, G. A. Voth, P. Salvador, J. J. Dannenberg, S. Dapprich, A. D. Daniels, Ö. Farkas, J. B. Foresman, J. V. Ortiz, J. Cioslowski and D. J. Fox, *Gaussian 09, Revision D.01*, Gaussian, Inc., Wallingford CT, 2009.
52 Y. Zhao and D. G. Truhlar, *Theor. Chem. Acc.*, 2008, **120**, 215–241.
53 C. M. Lausada, A. J. Johansson, T. Brinck and M. Johnson, *Phys. Chem. Chem. Phys.*, 2013, **15**, 5539–5552.
54 D. Andrae, U. Hausserman, M. Dolg, H. Stoll and H. Preuss, *Theor. Chim. Acta*, 1990, **77**, 123–141.
55 J. M. L. Martin and A. Sundermann, *J. Chem. Phys.*, 2001, **114**, 3408–3420.

